

Glueball enhancements in $p(\gamma, VV)p$ through vector meson dominance

Stephen R. Cotanch

Department of Physics, North Carolina State University, Raleigh, NC 27695-8202

Robert A. Williams

*Nuclear Physics Group, Hampton University, Hampton, VA 23668
and Jefferson Lab, 12000 Jefferson Ave, Newport News, VA 23606*

(Dated: May 3, 2019)

Double vector meson photoproduction, $p(\gamma, G \rightarrow VV)p$, mediated by a scalar glueball G is investigated. Using vector meson dominance (VMD) and Regge/pomeron phenomenology, a measurable glueball enhancement is predicted in the invariant $VV = \rho\rho$ and $\omega\omega$ mass spectra. The scalar glueball is assumed to be the lightest physical state on the daughter pomeron trajectory governing diffractive vector meson photoproduction. In addition to cross sections, calculations for hadronic and electromagnetic glueball decays, $G \rightarrow VV'$ ($V, V' = \rho, \omega, \phi, \gamma$), and $\gamma_v V \rightarrow G$ transition form factors are presented based upon flavor universality, VMD and phenomenological couplings from ϕ photoproduction analyses. The predicted glueball decay widths are similar to an independent theoretical study. A novel signature for glueball detection is also discussed.

PACS numbers: 12.39.Mk, 12.40.Nn, 12.40.Vv, 25.20.Lj

I. INTRODUCTION

Even though Quantum Chromodynamics (QCD) is the accepted theory of hadronic physics, realistic nonperturbative QCD predictions for reaction amplitudes are still not available. However, Quantum Hadrodynamics (QHD) calculations continue to provide a reasonable framework for the analysis of data. Related, the historical success of vector meson dominance (VMD) and Regge theory has led to an established legacy for investigating both electromagnetic and hadronic processes. Because of the wide interest in the gluonic aspects of QCD, especially glueballs, and new experimental opportunities at electromagnetic accelerator facilities, such as Jefferson Lab, this work combines QHD, VMD and Regge/pomeron physics to study double vector meson photoproduction, $p(\gamma, G \rightarrow VV)p$, mediated by a scalar glueball, G .

Central to our formulation is the pomeron-glueball hypothesis (PGH) [1, 2, 3] which connects the pomeron with the even signature $J^{PC} = 2^{++}, 4^{++}, \dots$ glueball Regge trajectory. Indeed both theoretical [1, 2, 3, 4, 5, 6] and experimental [7] evidence continues to accumulate which supports this conjecture. The PGH provides an attractive, logical framework for determining all glueball-hadron couplings from established pomeron phenomenology.

In this study we use the PGH to extend the effective Lagrangian model developed for ϕ photoproduction [8] and time-like virtual Compton scattering (TVCS) [9], to double vector meson photoproduction mediated by a scalar glueball. The necessary glueball-vector meson ($V = \rho, \omega, \phi$) hadronic and electromagnetic couplings are uniquely determined from PGH, VMD and isospin symmetry (flavor independence) of the glueball-hadron couplings. In addition to cross sections, we predict the $J^{PC} = 0^{++}$ glueball partial decay widths for double vector, $G \rightarrow VV'$, one photon, $G \rightarrow V\gamma$, and two photon,

$G \rightarrow \gamma\gamma$, decay channels. Since the vector meson leptonic decay constants are known, we also apply VMD to derive the radiative, $\gamma_v V \rightarrow G$, transition form factors required for scalar glueball electroproduction calculations. Our key finding is the prediction of a measurable $p(\gamma, G \rightarrow VV)p$ cross section and a glueball enhancement in the $\rho\rho$ and $\omega\omega$ invariant mass spectra near 1.7 GeV.

This paper spans six sections. In section II we review the essential features of ϕ electromagnetic production and TVCS [9] that are relevant for formulating VV photoproduction. Then we detail the QHD model in section III and in section IV present the VMD relations, glueball radiative transition form factors and decay widths. Section V contains our main results with theoretical $p(\gamma, VV)p$ cross sections documenting a measurable glueball enhancement and novel signature decay. Finally, in section VI we summarize and comment on future investigations.

II. ϕ PHOTOPRODUCTION AND TVCS MODEL SUMMARY

Vector meson photoproduction is known to be dominated by diffractive scattering at low momentum transfer and high energy. The diffractive amplitude has a clear exponential t -dependence, presumably generated by a tower of gluon t -channel exchanges, collectively known as the pomeron [10]. At low energy and for large momentum transfer, vector meson photoproduction is complicated by non-diffractive mechanisms such as pseudoscalar meson (π, η, η') exchange [8, 11], nucleon resonances and two-gluon exchange [12].

In ϕ photoproduction there are additional non-diffractive amplitudes due to strangeness knockout [13, 14] and Okubo-Zweig-Iizuka (OZI) [15] violating/evading ϕN couplings [8]. The ϕ photoproduction reaction is es-

pecially interesting for probing the intrinsic strangeness content of the nucleon [13, 14] and yields important constraints for the (off-shell) nucleon form factors in the vector meson resonance region accessible in TVCS, $\gamma p \rightarrow e^+ e^- p$ [9]. For example, OZI evading ϕN vector and tensor couplings contribute to the nucleon strangeness radius, strange magnetic moment and provide an improved description of the neutron electric form factor, $G_E^n(q^2)$ [16, 17, 18, 19, 20].

Our previous results documented that precision ϕ photoproduction and di-lepton TVCS data near the ϕ production threshold will provide important constraints for disentangling the complicated diffractive/non-diffractive amplitude components. In this work we apply the same effective Lagrangian used to calculate t -channel pomeron exchange in $p(\gamma, V)p$, to scalar glueball photoproduction $p(\gamma, G \rightarrow VV)p$. An important feature in the photoproduction/TVCS model is the photon-pomeron-vector meson vertex coupling associated with the t -channel pomeron exchange. Again we utilize this and now interchange the role of the pomeron and vector meson to consider t -channel ρ , ω and ϕ exchange leading to pomeron, or via the PGH, glueball photoproduction. We also interpret the scalar glueball as the $J = 0$ physical state on the daughter pomeron trajectory.

III. QHD MODEL DETAILS

We formulate the double vector meson photoproduction reaction as a two step mechanism mediated by a scalar glueball, G

$$\begin{aligned} \gamma(q, \lambda) + p(p, \sigma) &\longrightarrow p(p', \sigma') + G(q') \\ &\longrightarrow p(p', \sigma') + V(v_1, \lambda_1) + V'(v_2, \lambda_2) \end{aligned}$$

where the energy-momentum 4-vectors (helicities) for the photon, proton, glueball, recoil proton and vector mesons are given by q (λ), p (σ), $q' = v_1 + v_2$, p' (σ') and $v_{i=1,2}$ (λ_i), respectively. The general case is considered involving photoproduction of a glueball that may be on, $M_G = \sqrt{q'^2}$, or off-shell (virtual), $M_G \neq \sqrt{q'^2}$, and decays into two, possibly different, vector mesons $VV' = \rho\rho, \omega\omega, \phi\phi$ or $\omega\phi$ having masses $M_V = \sqrt{v_1^2}$, $M_{V'} = \sqrt{v_2^2}$. The 3-body final state differential cross section factorizes

$$\frac{d\sigma}{dt dM_{VV'}} = \frac{d\sigma_v}{dt} \mathcal{F}_{<VV'|G>} \quad (1)$$

where $M_{VV'} = \sqrt{q'^2}$ is the invariant VV' mass and $\frac{d\sigma_v}{dt}$ is the virtual glueball photoproduction cross section

$$\frac{d\sigma_v}{dt} = \frac{\pi}{\omega_{cm}^2} |< G p | \hat{T} | \gamma p >|^2. \quad (2)$$

The vector meson flux, $\mathcal{F}_{<VV'|G>}$, resulting from the glueball decay can be expressed in terms of phase space,

$\mathcal{P}_{VV'}$, the glueball propagator, $\Pi_G(q')$, and the $G \rightarrow VV'$ decay amplitude, $< VV'|G >$,

$$\mathcal{F}_{<VV'|G>} = \mathcal{P}_{VV'} | \Pi_G(q') |^2 | < VV'|G > |^2 \quad (3)$$

$$\mathcal{P}_{VV'} = \frac{|\mathbf{q}'|}{256\pi^4 M_p^2} \frac{\omega_{cm}^2}{\omega_{lab}^2} \quad (4)$$

$$\Pi_G(q'^2) = \frac{\sqrt{q'^2}}{q'^2 - M_G^2 + i\sqrt{q'^2} \Gamma_G} \left(\frac{s - s_{th}}{s_0} \right)^{\alpha_P(q'^2)} \quad (5)$$

$$< VV'|G > = \frac{g_{GVV'}}{2M_0} F_{\mu\nu}^V(v_1, \lambda_1) F_{V'}^{\mu\nu}(v_2, \lambda_2). \quad (6)$$

In these equations ω refers to the photon energy (in the appropriate frame), M_p is the proton mass, Γ_G is the glueball total width, $g_{GVV'}$ is the glueball-vector meson coupling constant, M_0 is a reference mass (set to 1 GeV) which permits a dimensionless glueball coupling and $F_{\mu\nu}^V$ is the vector meson current tensor specified below. The effective glueball propagator is a generalization of the empiracle space-like pomeron prescription [8] with the pole mass fixed at $M_G = 1.7$ GeV, consistent with the generally accepted lightest scalar glueball. Following Ref. [10], we have included in Eq. (5) the Regge factor, $(\frac{s-s_{th}}{s_0})^{\alpha_P(q'^2)}$, which describes the high energy behavior. Here $s = (q + p)^2$ is the usual cm energy Mandelstam variable and $\alpha_P(q'^2)$ is the pomeron trajectory of even signature glueballs with established linear form $\alpha_P(t) = \alpha_0 + \alpha't$. Because Regge theory only governs the asymptotic high energy behavior, we introduce the parameter, s_{th} ($0 \leq s_{th} \leq s_0$), to describe the low energy double meson production amplitude with the reference energy, $\sqrt{s_0}$, fixed at the threshold, $s_0 = (M_p + M_V + M_{V'})^2$. In previous, successful analyses of ϕ photoproduction using this prescription [8, 9] the available data clearly selected the maximum value, $s_{th} = s_0$, which is used through out this paper. If we omit the Regge factor the effective gluonic propagator takes a standard hadron (glueball) form and thus we loosely distinguish between pomeron (Regge) mediated or glueball (non-Regge) production. In section V we compare cross section predictions for both propagators.

In the helicity representation the glueball photoproduction amplitude, $< G p | \hat{T} | \gamma p >$, is

$$< G p | \hat{T} | \gamma p > = \epsilon_\mu(\lambda) \mathcal{H}_{\sigma'\sigma}^\mu, \quad (7)$$

where $\epsilon(\lambda)$ is the photon polarization 4-vector in the helicity basis and $\mathcal{H}_{\sigma'\sigma}^\mu$ is the hadronic current obtained by application of Feynman rules to the tree level s , $t = (q' - q)^2$ and $u = (p' - q)^2$ channel QHD diagrams. The hadronic current is evaluated in the total cm system ($\mathbf{q} + \mathbf{p} = \mathbf{q}' + \mathbf{p}' = 0$) with the z-axis taken along \mathbf{q} . In this frame the two photon polarization vectors are

$$\epsilon(\lambda) = -\frac{\lambda}{\sqrt{2}}(0, 1, i\lambda, 0) \quad (\lambda = \pm). \quad (8)$$

The $G(0^{++}) \rightarrow V(1^{--})V'(1^{--})$ decay helicity amplitude, $< VV'|G >$, involves the vector meson current

tensors $F_{\mu\nu}^V(v_1, \lambda_1)$ and $F_{V'}^{\mu\nu}(v_2, \lambda_2)$ given by

$$F_{\mu\nu}^V(v_i, \lambda_i) = v_{i\mu}\epsilon_{i\nu}(v_i, \lambda_i) - v_{i\nu}\epsilon_{i\mu}(v_i, \lambda_i) \quad (9)$$

with spin polarization 4-vectors, $\epsilon_i(v_i, \lambda_i)$, subject to the Lorentz condition $v_i \cdot \epsilon_i = 0$ for $i = 1, 2$. These polarization vectors satisfy

$$\sum_{\lambda_i} \epsilon_i^\mu(v_i, \lambda_i) \epsilon_i^{\nu*}(v_i, \lambda_i) = -g^{\mu\nu} + v_i^\mu v_i^\nu / M_i^2 \quad (10)$$

where $g_{\mu\nu} = g^{\mu\nu}$ is the standard metric tensor. The invariant helicity decay amplitude involves the contraction

$$F_{\mu\nu}^V F_{V'}^{\mu\nu} = 2(v_1 \cdot v_2 \epsilon_1 \cdot \epsilon_2 - v_1 \cdot \epsilon_2 v_2 \cdot \epsilon_1) \quad (11)$$

and can be evaluated in the glueball rest frame where, with \mathbf{v}_1 along the z-axis, the mesons 4-momenta are

$$v_1 = (E_1, \mathbf{v}_1) = (E_1, 0, 0, k_V) \quad (12)$$

$$v_2 = (E_2, \mathbf{v}_2) = (E_2, 0, 0, -k_V) \quad (13)$$

The 3-momentum $k_V = |\mathbf{v}_1| = |\mathbf{v}_2|$ depends on the vector meson and the glueball (invariant VV') masses

$$k_V = \frac{1}{2\sqrt{q'^2}} \left[(q'^2 + M_V^2 - M_{V'}^2)^2 - 4q'^2 M_V^2 \right]^{\frac{1}{2}} \quad (14)$$

In this frame the meson polarization vectors are

$$\epsilon_1(\lambda_1 = \pm) = -\frac{\lambda_1}{\sqrt{2}}(0, 1, i\lambda_1, 0) \quad (15)$$

$$\epsilon_1(\lambda_1 = 0) = \frac{1}{M_V}(k_V, 0, 0, E_1) \quad (16)$$

$$\epsilon_2(\lambda_2 = \pm) = -\frac{\lambda_2}{\sqrt{2}}(0, 1, i\lambda_2, 0) \quad (17)$$

$$\epsilon_2(\lambda_2 = 0) = \frac{1}{M_{V'}}(-k_V, 0, 0, E_2) \quad (18)$$

If the spins of the final state mesons are not detected, the cross section entails a helicity sum giving the factor

$$S \equiv \sum_{\lambda_1 \lambda_2=0, \pm 1} |< VV' | G >|^2 \quad (19)$$

$$= \frac{g_{GVV'}^2}{M_0^2} \sum_{\lambda_1 \lambda_2=0, \pm 1} [v_1 \cdot v_2 \epsilon_1(\lambda_1) \cdot \epsilon_2(\lambda_2) - v_1 \cdot \epsilon_2(\lambda_2) v_2 \cdot \epsilon_1(\lambda_1)]^2 \quad (20)$$

Using the above specific kinematical representation for v_i and ϵ_i or, more generally for any frame, Eq. (10), the summation reduces to the invariant result

$$S = \frac{g_{GVV'}^2}{M_0^2} [2(v_1 \cdot v_2)^2 + M_V^2 M_{V'}^2] \quad (21)$$

$$\rightarrow \frac{g_{GVV'}^2}{2M_0^2} [(M_{VV}^2 - 2M_V^2)^2 + 2M_V^4] (V = V') \quad (22)$$

The effective QHD Lagrangian for the strong and electromagnetic interactions generates the following

contributions to the hadronic current

t -channel $V = \rho, \omega, \phi$ exchange amplitudes:

$$\mathcal{H}_{\sigma'\sigma}^\mu = e g_{VNN} \frac{\kappa_{GV\gamma}}{M_0} F_t(t; \lambda_{cut}) \times \bar{u}(p', \sigma') [\gamma^\mu + i \frac{\kappa_V^T}{M_0} \sigma^{\mu\alpha} q'_\alpha] u(p, \sigma) \quad (23)$$

s -channel proton-glueball coupling amplitude:

$$\mathcal{H}_{\sigma'\sigma}^\mu = e g_{GNN} \bar{u}(p', \sigma') \frac{(p+q) \cdot \gamma + M_p}{s - M_p^2 + \Sigma_p(s)} \times [\gamma^\mu + i \frac{\kappa_p}{2M_p} \sigma^{\mu\beta} q_\beta] u(p, \sigma) \quad (24)$$

u -channel proton-glueball coupling amplitude:

$$\mathcal{H}_{\sigma'\sigma}^\mu = e g_{GNN} \bar{u}(p', \sigma') [\gamma^\mu + i \frac{\kappa_p}{2M_p} \sigma^{\mu\beta} q_\beta] \times \frac{(p' - q) \cdot \gamma + M_p}{u - M_p^2 + \Sigma_p(u)} u(p, \sigma) \quad (25)$$

Here $e = \sqrt{4\pi\alpha_e}$ and each hadronic current term has an effective coupling strength involving a glueball hadronic or electromagnetic coupling constant. The factor κ_V^T in Eq. (23) is the tensor to vector coupling constant ratio for the ρ, ω or ϕ nucleon vertex and $\kappa_p = 1.793$ is the proton anomalous magnetic moment.

In the t -channel the hadronic form factor, $F_t(t; \lambda_{cut})$, incorporates the composite nucleon and vector meson structure which can be calculated in constituent quark models and is important for regulating the energy and momentum transfer dependence in meson photoproduction [21, 22]. However, to preserve the covariance and crossing properties of our model, we employ the phenomenological form factor [8, 9]

$$F_t(t; \lambda_{cut}) = \frac{\lambda_{cut}^4 + t_{min}^2}{\lambda_{cut}^4 + t^2}, \quad (26)$$

normalized to unity at $t_{min} = t(\theta_{\gamma G}^{cm} = 0)$. Fitting the $p(\gamma, \phi)p$ data yields the optimum cut-off parameter $\lambda_{cut} = 0.7$ GeV. Also note that, unlike vector meson electromagnetic production, for t -channel $J^{PC} = J^{++}$ glueball (pomeron) production, pseudoscalar meson exchange is prohibited by C -parity conservation. Hence π exchange only contributes to the production of $C = \text{odd}$ glueball states which have much higher masses and are also more difficult to detect.

In the s and u -channels, the highly virtual proton propagation requires an off-shell form factor prescription. Because the s and u -channel diagrams must combine to produce a conserved hadronic current, we incorporate the off-shell effect as a self-energy correction. Constrained by gauge invariance and the proton mass, the self-energy function must vanish at the proton pole and also be an odd function of $s - M_p^2$. Hence we take

$$\Sigma_p(s) = \alpha_{off} \frac{(s - M_p^2)^3}{M_p^4} \quad (27)$$

The dimensionless off-shell parameter, $\alpha_{off} = 1.29$, was determined by fitting recent ϕ photoproduction data [23].

The model parameters for the pomeron amplitude are listed in Table I and the vector meson coupling constants are specified in Table II. The glueball-vector meson couplings are assumed to be flavor independent (*universality* hypothesis) due to isospin/flavor invariance of gluonic interactions.

TABLE I: Pomeron/glueball hadronic coupling and Regge trajectory, $\alpha(t) = \alpha_0 + \alpha' t$, parameters.

g_{GNN}	$g_{GVV'}$	α_0	$\alpha' (GeV^{-2})$
44.0	3.43	1.0	0.27

TABLE II: Vector meson coupling constants.

$g_{\rho NN}$	$g_{\omega NN}$	$g_{\phi NN}$	κ_ρ^T	κ_ω^T	κ_ϕ^T
2.014	3.411	1.306	6.100	0.140	1.820

IV. GLUEBALL DECAY WIDTHS AND TRANSITION FORM FACTORS

In this section we present our VMD formulation for the proton, vector meson and glueball transition form factors. In our previous ϕ photoproduction/TVCS calculations we utilized a hybrid VMD approach [19, 20] that was a generalization of the model developed by Gari and Krümpelmann [18]. This formalism incorporates $SU_F(3)$ symmetry relations and Sakurai's universality hypothesis to describe the baryon octet EM form factors, predominantly constrained by nucleon data. Our treatment provided a good quantitative description of the data using the vector meson-nucleon couplings, $C_\rho(N) = 0.4$, $C_\omega(N) = 0.2$ and $C_\phi(N) = -0.1$ (see Ref. [19] where the value of $C_\phi(N)$ was optimized to describe G_E^n data). Here $C_V(N) = g_{VNN}/f_V$ is the ratio of the vector meson-nucleon hadronic coupling, g_{VNN} , to the vector meson-leptonic decay constant, f_V . Using

$$\Gamma_{V \rightarrow e^+e^-} = \frac{4\pi\alpha_e^2}{3} \frac{M_V}{f_V^2} \quad (28)$$

for the $\phi \rightarrow e^+e^-$ decay yields, $f_\phi = -13.1$, giving the ϕN coupling $g_{\phi NN} = 1.3$. Recent, preliminary G_E^n measurements from Jefferson Lab indicate a reduction at higher momentum compared to previous data, which suggests an even larger ϕN coupling. Although there is uncertainty in $g_{\phi NN}$, which is governed by the currently unknown nucleon strangeness content (as well as the small, but better known, u and d quark content of the ϕ), the value $g_{\phi NN} = 1.3$ accurately reproduces [9] both old, low, and new, high, t ϕ photoproduction data.

The ratio of the ϕN to the ωN coupling constant is $g_{\phi NN}/g_{\omega NN} = 0.37$, slightly smaller but still consistent with Ref. [24].

The $\gamma\pi \rightarrow \gamma_v$, $\gamma\eta \rightarrow \gamma_v$ and $\gamma G \rightarrow \gamma_v$ transition form factors are computed from VMD using the vector meson propagators, $\Pi_{V=\rho,\omega,\phi}(q^2)$, with observed widths, Γ_V ,

$$\Pi_V(q^2) = -\frac{M_V^2}{q^2 - M_V^2 + i\sqrt{q^2} \Gamma_V} \quad (29)$$

and couplings determined directly from the $\phi \rightarrow \gamma\pi$, $\phi \rightarrow \gamma\eta$, $\omega \rightarrow \gamma\pi$, $\omega \rightarrow \gamma\eta$, $\rho \rightarrow \gamma\pi$ and $\rho \rightarrow \gamma\eta$ decays

$$\Gamma_{V \rightarrow X\gamma} = \frac{\alpha_e}{3} \frac{k_X^3}{M_0^2} \kappa_{XV\gamma}^2 \quad (30)$$

for $X = \pi, \eta$ and G . Again the mass, $M_0 = 1.0$ GeV, is an arbitrary scale in the $XV\gamma$ Lagrangian and k_X is the rest frame 3-momentum of the decay particles, given by a relation identical to Eq. (14). VMD then yields

$$\kappa_{\pi\gamma\gamma} F_{\gamma\pi \rightarrow \gamma_v}(q^2) = \sum_{V=\rho,\omega,\phi} C_{\pi V\gamma} \Pi_V(q^2) \quad (31)$$

$$\kappa_{\eta\gamma\gamma} F_{\gamma\eta \rightarrow \gamma_v}(q^2) = \sum_{V=\rho,\omega,\phi} C_{\eta V\gamma} \Pi_V(q^2) \quad (32)$$

$$\kappa_{G\gamma\gamma} F_{\gamma G \rightarrow \gamma_v}(q^2) = \sum_{V=\rho,\omega,\phi} C_{GV\gamma} \Pi_V(q^2), \quad (33)$$

where the dimensionless C -coefficients are ratios of transition moments and decay constants

$$C_{\pi V\gamma} = \frac{\kappa_{\pi V\gamma}}{f_V} \quad (34)$$

$$C_{\eta V\gamma} = \frac{\kappa_{\eta V\gamma}}{f_V} \quad (35)$$

$$C_{GV\gamma} = \frac{\kappa_{GV\gamma}}{f_V}. \quad (36)$$

The pomeron/glueball radiative and transition decay constants are not directly known, however they have been indirectly extracted from ϕ photoproduction data and the VMD/universality relation [8, 9]

$$\kappa_{GV\gamma} = g_{GVV'} \left[\frac{1}{f_\rho} + \frac{1}{f_\omega} + \frac{1}{f_\phi} \right] = 0.62. \quad (37)$$

Using the most recently measured vector meson radiative and leptonic decay widths [25], we obtain the VMD coupling constants summarized in Table III.

The pseudoscalar $\pi \rightarrow \gamma\gamma$ and $\eta \rightarrow \gamma\gamma$ radiative decay widths

$$\Gamma_{X \rightarrow \gamma\gamma} = \frac{\pi\alpha_e^2}{4} \frac{M_X^3}{M_0^2} \kappa_{X\gamma\gamma}^2, \quad (38)$$

provide a VMD consistency check for the π and η transition form factors, Eqs. (31) and (32), due to the normalization conditions ($F_{\gamma\pi \rightarrow \gamma_v}(0) = 1$, etc.)

$$\kappa_{\pi\gamma\gamma} = \frac{\kappa_{\pi\rho\gamma}}{f_\rho} + \frac{\kappa_{\pi\omega\gamma}}{f_\omega} + \frac{\kappa_{\pi\phi\gamma}}{f_\phi} \quad (39)$$

$$\kappa_{\eta\gamma\gamma} = \frac{\kappa_{\eta\rho\gamma}}{f_\rho} + \frac{\kappa_{\eta\omega\gamma}}{f_\omega} + \frac{\kappa_{\eta\phi\gamma}}{f_\phi}. \quad (40)$$

TABLE III: VMD couplings from measured decays [25]. The flavor independent glueball couplings are from Refs. [8, 9].

V	$\kappa_{\pi V\gamma}$	$\kappa_{\eta V\gamma}$	$\kappa_{GV\gamma}$	f_V
ρ	0.901	1.470	0.62	5.0
ω	2.324	0.532	0.62	17.1
ϕ	0.138	0.715	0.62	-13.1

Using recent data [25] we obtain excellent agreement between experiment and the VMD predictions

$$\begin{aligned} \text{experiment [Eq. (38)] : } & \quad \kappa_{\pi\gamma\gamma} = 0.27 \quad \kappa_{\eta\gamma\gamma} = 0.26 \\ \text{VMD [Eqs. (39, 40)] : } & \quad \kappa_{\pi\gamma\gamma} = 0.30 \quad \kappa_{\eta\gamma\gamma} = 0.27 . \end{aligned}$$

The glueball hadronic widths, using

$$\Gamma_{G \rightarrow VV} = \frac{g_{GVV}^2}{4\pi} \frac{k_V^3}{M_0^2}, \quad (41)$$

are listed in Table IV. The notation N/A indicates not allowed by isospin conservation, while N/P represents insufficient phase space. It is noteworthy that the $G \rightarrow \rho\rho$ and $\omega\omega$ widths of 44.4 and 34.6 MeV reasonably compare to predictions from an independent glueball mixing and decay analysis [26] which predicts 46 and 12 MeV, respectively. The electromagnetic widths, using Eq. (30), are presented in Table V. The vector meson photon decay widths are also shown for comparison.

We can also calculate the glueball 2-photon radiative decay width by first evaluating Eq. (33) for $q^2 = 0$,

$$\kappa_{G\gamma\gamma} = \kappa_{GV\gamma} \left[\frac{1}{f_\rho} + \frac{1}{f_\omega} + \frac{1}{f_\phi} \right] = 0.11 \quad (42)$$

where again universality is invoked for all V . The VMD prediction from Eq. (38) for the $G \rightarrow \gamma\gamma$ decay width is then, $\Gamma_{G \rightarrow \gamma\gamma} = 2.6$ eV, which is comparable to the meson decay widths $\Gamma_{\pi \rightarrow \gamma\gamma} = 7.74$ eV and $\Gamma_{\eta \rightarrow \gamma\gamma} = 0.46$ eV.

Combining the above values yields a total hadronic VV scalar glueball width of 79 MeV which of course only represents a lower bound for the full width. Indeed there are several other decay channels involving lighter mesons (π, η, K, a_1) which will compete and Ref. [26] estimates the total width could be up to 250 MeV. The actual width is between these two limits and probably closer to the observed widths for the $f_0(1500)$ and $f_0(1710)$ glueball candidates which are 109 and 125 MeV, respectively.

TABLE IV: VMD glueball hadronic decay widths in MeV.

$\Gamma_{G \rightarrow VV'}$	ρ	ω	ϕ
ρ	44.4	N/A	N/A
ω	N/A	34.6	N/P
ϕ	N/A	N/P	N/P

TABLE V: VMD glueball electromagnetic decays in eV.

$V \rightarrow$	ρ	ω	ϕ
$\Gamma_{G \rightarrow V\gamma}$	866	844	454
$\Gamma_{V \rightarrow \pi\gamma}$	102	717	6
$\Gamma_{V \rightarrow \eta\gamma}$	36	6	59

Finally, glueball electroproduction via intermediate virtual photons will require form factors for the transition $\gamma_v V \rightarrow G$. Again, simple application of VMD yields the appropriate $\gamma_v V \rightarrow G$ transition form factors

$$\kappa_{GV\gamma} F_{\gamma V \rightarrow G}(q^2) = \sum_{V'=\rho,\omega,\phi} \frac{g_{GVV'}}{f_{V'}} \Pi_{V'}(q^2). \quad (43)$$

V. CROSS SECTION PREDICTIONS

This section summarizes the key cross section findings and presents results for a variety of kinematics. Figure 1 displays the exclusive photoproduction cross section versus the VV invariant mass. The three solid curves, corresponding to different glueball widths, represent production and decay to the $\rho\rho$ or $\omega\omega$ final states. Because of universality ($g_{G\rho\rho} = g_{G\omega\omega}$) and the near degeneracy of the ρ and ω masses, the $\rho\rho$ and $\omega\omega$ production cross sections are essentially equal so one curve represents both channels. The two short dashed curves are for $\phi\phi$ production which has a higher threshold.

The long dashed curve is the non-Regge prediction using $\Gamma_G = 79$ MeV. This is the result using the gluonic propagator without the Regge factor and, as discussed previously, can be regarded as production mediated by more conventional hadron (glueball) formation. Notice that it is about a factor of 4 larger than the Regge (pomeron) prediction using the same width (top solid line). A similar increase occurs for the two other widths (not shown).

To document sensitivity to the uncertain glueball width, three values are displayed. The upper solid curve depicting the distinct resonant glueball structure assumes that vector meson decay saturates the entire glueball width and uses the value $\Gamma_{G \rightarrow VV} = \Gamma_{G \rightarrow \rho\rho} + \Gamma_{G \rightarrow \omega\omega} = 79$ MeV from Table IV. The lower curve corresponds to a width of 238 MeV which is taken as an upper bound and is also the numerical width necessary to completely suppress the glueball cross section enhancement. The middle curve uses $\Gamma_G = 125$ MeV which, as discussed in section IV, is probably closer to the physical glueball value. Hence, if the actual width is roughly of order 100 MeV, a clear glueball enhancement can emerge.

The two dashed $\phi\phi$ production curves, corresponding to the minimum and maximum glueball widths, are essentially the same since the $\phi\phi$ threshold is well above the on-shell glueball mass ($M_G = 1.7$ GeV) and only a small effect is present from the off-shell gluonic propagator. Consequently $\phi\phi$ production is predicted to be

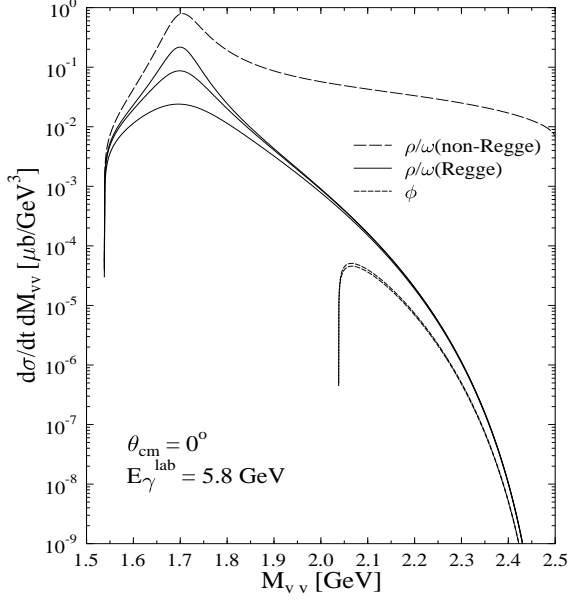


FIG. 1: Cross sections for $p(\gamma, G \rightarrow VV)p$ vs. the invariant VV mass. Solid lines represent the $\rho\rho$ (or $\omega\omega$) cross sections for different glueball widths. The short dashed curves represent $\phi\phi$ photoproduction. The long dashed curve omits the Regge energy dependence.

devoid of a light scalar glueball enhancement. This is also why the $\rho\rho$ (or $\omega\omega$) curves converge at higher invariant VV mass, a region of interests for effects from a tensor, $J^{PC} = 2^{++}$, glueball that is expected to have mass near 2 GeV. Related, Ref. [25] lists several f_2 , possible glueball, states above 2 GeV with observed $\phi\phi$ decays.

The cross section kinematics reflect the capability of the envisioned Hall D facility at Jefferson Lab. Depending on choice of gluonic propagator, there is sensitivity to the incident photon energy as indicated in Fig. 2. While the energy behavior of the non-Regge prediction (dashed line) is relatively flat, the Regge calculation (solid curve) increases with higher beam energy. There is little energy or s dependence in the non-Regge calculation since the cross section is at forward angles (t -channel dominated). Because the Regge formulation is more phenomenologically based, it is our preferred prediction. However, it would be interesting to confront both results with multiple vector meson production data at low and high energies. Interestingly, the two formulations yield similar cross sections (and measurable production rates) near 7 GeV which is a frequently cited Jlab upgraded photon energy. Hence it should be feasible to confirm the gluonic enhancement predicted in Fig. 1.

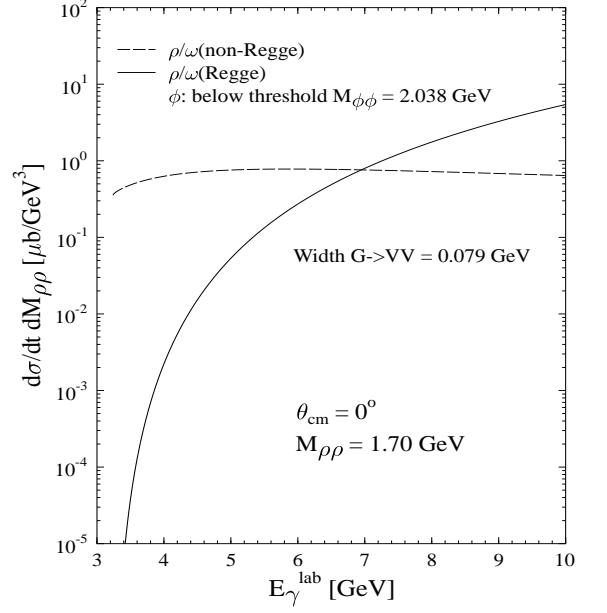


FIG. 2: Comparison of Regge (pomeron, solid line) and non-Regge (glueball, dashed line) mediated production vs. lab energy.

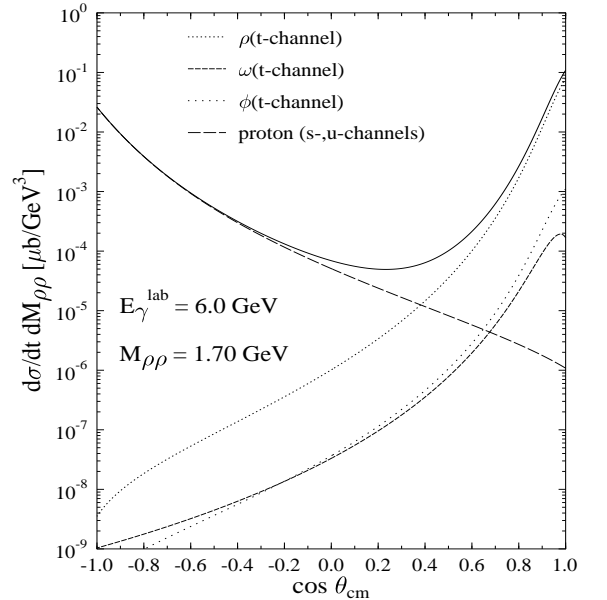


FIG. 3: Relative s , t and u -channel contributions.

There is significant sensitivity to the production final state angle, θ_{cm} , or momentum transfer. This is reflected in Fig. 3 which details a falling, then rising cross section with increasing angle. Note the minimum cross section occurs for $\theta_{cm} = 90^\circ$. This prediction is for $E_\gamma^{lab} = 6.0$ GeV and corresponds to the intermediate, more representative glueball width. As expected for small angles (low t) t -channel vector meson exchange dominates with ρ exchange (dense dot curve) being the most important. At larger angles (higher t) s and u -channel amplitudes emerge (dashed curve) corresponding to production from glueball-proton coupling. Because both s and q' are fixed, the Regge and non-Regge (not shown) results have identical t -channel relative contributions and variations.

It is important to relate these predictions to the expected background VV production from non-glueball mediated processes. Unfortunately, to our knowledge there are no specific model calculations in this energy region. However, other double meson photoproduction calculations exist and Refs. [27, 28] predict cross sections comparable in magnitude to those calculated here. Further, Ref. [27] investigates possible exotic, $J^{PC} = 1^{-+}$, meson excitation in $\gamma p \rightarrow \rho^0 \pi^+ n$ and predicts a similar resonance profile to our glueball production result.

Finally, we note a novel detection signature predicted by this analysis. Because of the dominant $\rho \rightarrow \pi\pi$, $\omega \rightarrow \pi\pi\pi$ and $\phi \rightarrow KK$ decays, the presence of a glueball excitation should be correlated with a 4 and 6 π decay around 1.7 GeV in the invariant $\rho\rho$ and $\omega\omega$ mass spectra, respectively. Further, and depending on the proximity of the glueball mass to the $\omega\phi$ threshold, there also may be a $\pi^+\pi^-\pi^0 K^+K^-$ decay near or above 1.8 GeV in the $\omega\phi$ spectrum. The latter may be a unique signature as there are no hadrons listed with this decay. This would be an ideal experiment for the envisioned Hall D large acceptance spectrometer.

VI. CONCLUSIONS

This work combines the time-honored tools of Quantum Hadrodynamics, vector meson dominance and Regge theory with the pomeron-glueball connection hypothesis to predict glueball production and decay processes. Using a minimal set of parameters independently determined from recent hadronic and electromagnetic analyses, a measurable cross section is predicted for $p(\gamma, G \rightarrow VV)p$. Most significant is a possible scalar glueball enhancement near 1.7 GeV in the $\rho\rho$ and $\omega\omega$ invariant mass spectra. This resonant cross section structure is sensitive to the total glueball width and should be discernable if the width is of order 100 MeV. If the actual width is significantly larger, say greater than 200 MeV, it may still be possible to detect a scalar glueball via decay to either 4 or 6 pions having an invariant mass near 1.7 GeV. Even more novel would be a correlated $\pi^+\pi^-\pi^0 K^+K^-$ observation in this same mass region, which would be a unique decay signature from a scalar hadron. Such measurements would be ideal for the envisioned JLab energy upgrade and new Hall D wide acceptance spectrometer.

Future work will address other scalar glueball decay channels. Related, tensor glueball production and decay will be investigated which will be especially interesting since the 2^{++} glueball mass is expected to be above the clear signature $\phi\phi$ decay threshold.

Acknowledgments

This work was supported by the Department of Energy under grant DE-FG02-97ER41048.

-
- [1] F. J. Llanes-Estrada, S. R. Cotanch, P. Bicudo, E. Ribeiro, and A. P. Szczepaniak, Nucl. Phys. **A710**, 45 (2002).
 - [2] S. R. Cotanch, Prog. Part. Nucl. Phys. **50**, 353 (2003).
 - [3] S. R. Cotanch, Nucl. Phys. **A**, *in press* (2004).
 - [4] L. Kisslinger and W. Ma, Phys. Lett. B **485**, 367 (2000).
 - [5] D. Q. Liu and J. M. Wu, hep-lat/0105019 (2002).
 - [6] H. B. Meyer and M. Teper, hep-lat/0306019 (2003).
 - [7] N. I. Kochelev *et al.*, Phys. Rev. D **67**, 074014 (2003).
 - [8] R. A. Williams, Phys. Rev. C **57**, 223 (1998).
 - [9] S. R. Cotanch and R. A. Williams, Phys. Lett. B **549**, 85 (2002).
 - [10] P. D. B. Collins, *An Introduction to Regge Theory and High Energy Physics* (Cambridge University Press, Cambridge, 1977).
 - [11] M. A. Pichowsky, Ph.D. Thesis, University of Pittsburg (1996).
 - [12] J. M. Laget *et al.*, Jefferson Lab experiment E-93-031.
 - [13] E. M. Henley, G. Krein, S. J. Pollock, and A. G. Williams, Phys. Lett. B **269**, 31 (1991); E. M. Henley, G. Krein, and A. G. Williams, Phys. Lett. B **281**, 178 (1992).
 - [14] A. I. Titov, S. N. Yang, and Y. Oh, Nucl. Phys. **A618**, 259 (1997); A. I. Titov, Y. Oh, and S. N. Yang, Phys. Rev. Lett. **79**; A. I. Titov, Y. Oh, S. N. Yang, and T. Morii, Phys. Rev. C **58**, 2429 (1998).
 - [15] S. Okubo, Phys. Lett. **5**, 165 (1963); G. Zweig, CERN Report No. 8419/TH412 (1964); I. Iizuka, Prog. Theor. Phys. **38**, 21 (1966).
 - [16] G. Hohler *et al.*, Nucl. Phys. **B114**, 505 (1976).
 - [17] S. Dubnicka, Nuovo Cim. **A100**, 1 (1988).
 - [18] M. Gari and W. Krumpelmann, Phys. Lett. B **274**, 159 (1992).
 - [19] R. A. Williams, S. Krewald, and K. Linen, Phys. Rev. C **51**, 566 (1995).
 - [20] R. A. Williams and C. Puckett-Truman, Phys. Rev. C **53**, 1580 (1996).
 - [21] Z. Li, Phys. Rev. C **52**, 1648 (1995).
 - [22] D. Lu, R. H. Landau, and S. C. Phatak, Phys. Rev. C **52**, 1662 (1995).
 - [23] CLASS Collaboration, E. Anciant, *et al.*, Phys. Rev.

- Lett. **85**, 4682 (2000).
- [24] J. Ellis, E. Gabathuler, and M. Karliner, Phys. Lett. B **217**, 173 (1989).
- [25] K. Hagiwara *et al.*, Phys. Rev. D **66**, 010001 (2002).
- [26] L. Burakovsky and P. R. Page, Phys. Rev. D **59**, 014022 (1999).
- [27] A. V. Afanasev and A. P. Szczepaniak, Phys. Rev. D **61**, 114008 (2000).
- [28] L. Bibrzycki, L. Lesniak, and A. P. Szczepaniak, hep-ph/0308267.